A modification of nonlinear Forchheimer's coefficient for fracture flow during shear

Min Gao
School of Minerals and Energy Resources Engineering, University of New South Wales, Sydney, Australia

Xu Zhu
School of Minerals and Energy Resources Engineering, University of New South Wales, Sydney, Australia

Chengguo Zhang
School of Minerals and Energy Resources Engineering, University of New South Wales, Sydney, Australia

Joung Oh
School of Minerals and Energy Resources Engineering, University of New South Wales, Sydney, Australia

ABSTRACT: This study introduces a new hydromechanical model to estimate both shear and nonlinear flow behaviours of a single rock fracture, taking into account the effects of fracture surface morphology on the fracture flow behaviours. The model incorporates a multi-scale roughness shear constitutive model that considers the adhesion and abrasion wear theories to predict the shear behaviours of a fracture due to shear deformations. The fracture permeability is estimated using the Forchheimer-based equation, which accounts for the combined effects of the fracture void spaces, aperture distributions, and fluid flow tortuosity. Laboratory shear-flow experiments under different hydraulic pressures and normal loading conditions are conducted to validate the proposed model. The model is in good agreement with experimental data and can be applied to sheared aquifers.

Keywords: Shear-flow model, single fracture, surface roughness, multi-scale roughness, nonlinear flow.

1 INTRODUCTION

Fluid flow through rock fracture is a crucial issue in seepage-related engineering projects and has been extensively studied over a few decades (Olsson and Barton, 2001, Xiong et al., 2011, Rong et al., 2018, Wang et al., 2020). One of the simplest conceptual models to estimate fracture permeability is the cubic law, which assumes that the fracture consists of two smooth and parallel plates. This model is valid for low flow rate conditions and states that the fracture flow rate is proportional to the cube of the fracture aperture, as proposed by Witherspoon et al. (1980).

In a shear process, the evolutions of fracture surface morphology result in the occurrence of nonlinear flow. Experimental observations show that the linear cubic law deviates from the nonlinear flow behaviours with increasing applied water pressures and inhomogeneity of surface geometries (Rong et al., 2018). However, only a few models have been developed to estimate shear-flow behaviours of a fracture. Olsson and Barton (2001) estimated shear behaviour using the Barton-Bandis shear model and hydraulic behaviour using modified cubic law. Later, Rong et al. (2018) extended this model to solve the nonlinear fracture flow by a Forchheimer-based equation. However, determining a unique *JRC* value on an irregular fracture is difficult. Besides, a single *JRC* or JRC_{mob}

cannot explain the influences of complex surface morphology, e.g., various aperture, contact distributions, and flow tortuosity, on fracture flow behaviours. Xiong et al. (2011) developed a flow model to predict the fracture hydraulic properties during shearing. They proposed an empirical equation between mechanical aperture e_m and hydraulic aperture e_h by considering the mean and standard deviations of the local apertures, which were estimated by a fracture void space model. However, the fluid flow governing equation is the cubic law, which has limitations in solving nonlinear fracture flow problems.

To address these limitations, this study proposes a new step-wise hydromechanical model consisting of a mechanical unit, a fracture void space model, and a hydraulic unit. The model employs a multi-scale roughness shear constitutive model to estimate the shear mechanical behaviours of the fracture. The fracture void space model is used to determine aperture distribution, relative roughness, fluid flow tortuosity, and fracture surface tortuosity. These parameters are then incorporated into the Forchheimer-based equation to predict the fracture discharge. Laboratory shear-flow tests are conducted under normal stress to verify the proposed model. The results of the tests demonstrate a strong agreement between the proposed model and experimental data.

2 EXPERIMENTAL PROCESS AND MODEL DEVELOPMENT

2.1 Experimental process

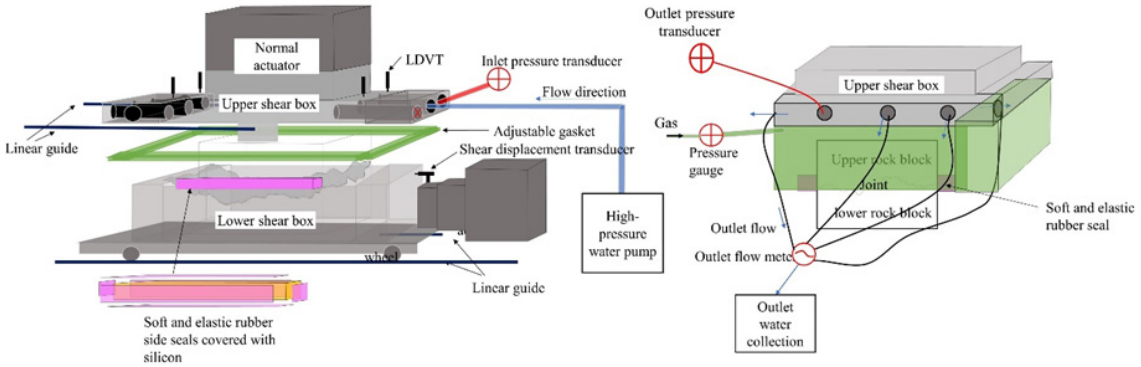

Figure 1. Schematic of the shear-flow test devices.

An artificial fracture *S1* (*JRC*=8-10 visually measured) was created by splitting an intact Gosford sandstone at the mid-height. The fracture specimens were replicas of *S1* and were made of water and Epirez Class A Superstrength Grout in a weight ratio of 0.2 (uniaxial compressive strength of a fully saturated specimen *UCS* 29MPa, basic friction angle ϕ_b 28°). The upper fracture had a length (L),and width (w), and height 100mm*100mm*50mm, while the lower fracture was extended by 13 mm in length. The fracture was placed in the shear boxes without any initial shearing. During the tests, the upper shear box moved vertically, and simultaneously, the lower shear box moved horizontally at a constant shear rate of 5mm/min. Normal displacements of the specimens were measured by four linear variable differential transducers (LDVTs) (as shown in Figure 1). The shear and normal loads and shear and normal displacements are recorded automatically by the loggers. A high-water pressure pump continuously supplied water with constant water pressure into the fracture, and the inlet water pressure was recorded by a pressure transducer. The fracture discharge over the fracture was collected through six interconnected drill holes. A pressure transducer measured the outlet water pressure and was used to estimate the fracture differential pressure. A silicon rubber gasket and two soft and elastic rubber were used to prevent water leakages from the specimens. In all the shear-flow tests, the outlet water pressures were closed to zero (Wang et al., 2020), indicating good sealing performance of the shear-flow testing system.

2.2 Model implementation

A schematic of the proposed hydromechanical model implementation is presented in Figure 2, including three calculation stages: mechanical, fracture void space, and hydraulic calculations. Shear stresses and shear deformations are updated at each incremental shear displacement (du_s), and normal displacement is utilised in the fracture void space model to estimate the aperture distribution and relative surface roughness parameters. The fracture discharge is predicted at the end of each calculation circle by the Forchheimer equation.

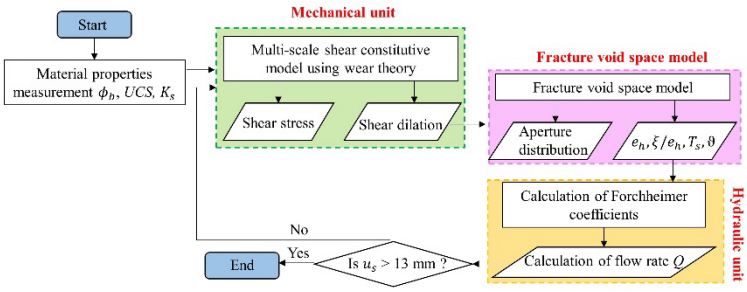

Figure 2. Solution framework of hydromechanical model implementation.

2.2.1 Shear mechanical model

The shear behaviours of a fracture are estimated by a multi-scale roughness continuously yielding constitutive model proposed by Gao et al. (2023). The fracture surface roughness of *S1* is quantified by two laboratory-scale roughness: laboratory-scale waviness and unevenness (the laboratory-scale waviness is 77.63 mm in wavelength (λ_p) and 7.39° in inclination angle (a_p), and unevenness is 6.34 mm in wavelength (λ_s) and 14.38° in inclination angle(a_s)). Shear stress is estimated by separating the asperity shearing from the basic friction sliding component, which is supported by strong theoretical foundations. The elastic and pre-peak softening stages are predicted using Eq. (1), while Eq. (2) describes the post-peak softening behaviour. The reduction of shear strength due to the degradation of surface asperity is modelled using the adhesion and abrasion wear theories (details are presented in Gao et al. (2023)).

$$\tau_i = \tau_{i-1} + \int F_i * k_s * du_s \tag{1}$$

$$\tau = \sigma_n \tan(\psi_{mob} + \phi_b) + \sigma_n \frac{\mu_{mob}}{1 - \tan(\psi_{mob})\tan(\phi_b)} \tag{2}$$

where τ_i and τ_{i-1} are the shear stresses at i^{th} and $i-1^{\text{th}}$ time-step, F_i is the reduction factor, k_s is the shear stiffness, σ_n is normal stress, ψ_{mob} and μ_{mob} are the mobilised dilation and asperity shearing components.

2.2.2 Fracture void space model

The mechanical aperture during shear is calculated by Eq. (3) (Esaki et al., 1999). Under constant normal loading conditions, d_n is equal to zero, and d_s is estimated by the shear constitutive model (section 2.2.1). The initial mechanical aperture e_o is assumed to be equal to initial hydraulic aperture, which is obtained by back analysing the shear-flow data (Xiong et al., 2011).

$$e_m = e_o - d_n + d_s \tag{3}$$

The evolution of the fracture void space evolution is computed at each u_s by fixing the lower fracture and moving the upper fracture horizontally (with u_s) and vertically (with d_s). The local aperture is measured as the distance between the upper and lower surface at each point (x_i, y_i), and the contact is when the local aperture is less or equal to zero (Xiong et al., 2011). As the fracture flow behaviour is associated with various local-scale apertures (Xiong et al., 2011), e_h is estimated by incorporating the standard deviation (σ_{ape}) and mean ($\langle e_m \rangle$) of the aperture using Xiong's empirical equation.

2.2.3 Forchheimer Coefficients

The Forchheimer equation (Eq. 4) depicts the nonlinear fracture flow, where *A* and *B* are the linear and nonlinear coefficients, respectively.

$$-\nabla P = AQ + BQ^2 = 12\frac{\mu}{e_h^3 w}Q + b_D\frac{\rho}{e_h^3 w^2}Q^2 \tag{4}$$

where ρ is water density, μ dynamic viscosity, and b_D is a dimensionless nonlinear factor.

The presents of fracture-inherent asperities and inhomogeneous obstructions (contacts or gouge particles) enhance the inertia effect of the fluid flow, deviating the fluid flow from linearity. Three parameters: a relative roughness (ξ/D_h), flow tortuosity (ϑ), and joint surface tortuosity (T_s) are introduced into b_D(see Eq. (5)) to explain the impacts of surface roughness on fluid flow behaviours. These parameters are obtained from the fracture void space model.

$$b_D = \frac{1}{11} * \left(log\left(\frac{\xi}{2e_h}\right)\right)^{-2} * T_s^2 * \vartheta^2 \tag{5}$$

Several previous studies (Chen et al., 2015) applied $log(\xi/2e_h)$ (ξ, peak asperity height) to b_D, as the peak asperities control both mechanical and hydraulic behaviours of a fracture. To further consider the impacts of surface roughness and fluid flow tortuosity on fracture flow behaviours, T_s and ϑ are introduced into b_D. T_s is the fracture tortuosity and is written as Eq. (6), and ϑ is tortuosity and is written as Eq. (7), according to Xiao et al, (2013)**.**

$$T_s^m = \frac{\Delta x \Delta y}{wL}\sum_{x_i=1}^{N_x-1}\sum_{y_j=1}^{N_y-1}\sqrt{1+\left(\frac{z_{x_{i+1},y_j}-z_{x_i,y_j}}{\Delta x}\right)^2+\left(\frac{z_{x_i,y_{j+1}}-z_{x_i,y_j}}{\Delta y}\right)^2} \tag{6}$$

where N_x and N_y are the number of points along the x and y directions (y is the shear direction, x is fracture width), Δx and Δy are 0.2 mm. z_{x_i,y_j}, z_{x_{i+1},y_j} and $z_{x_i,y_{j+1}}$ are the asperity height at point (x_i, y_j), (x_{i+1}, y_j) and (x_i, y_{j+1}). m is either *u* or *l,* indicating the upper or lower fracture surface. T_s is the average value of the upper and lower surface.

$$\vartheta_k = \frac{\sum_{y_j=1}^{N_y-1}\sqrt{(\Delta y)+\left(e_{x_i,y_{j+1}}-e_{x_i,y_j}\right)^2}}{\mathrm{L}} \tag{7}$$

where *k* is k^{th} flow path, *N* is the total number of selected flow paths. $e_{x_i,y_{j+1}}$ and e_{x_i,y_j} are the local mechanical apertures at points z_{x_i,y_j} and $z_{x_i,y_{j+1}}$

3 MODEL PERFORMANCE AND VERIFICANTION

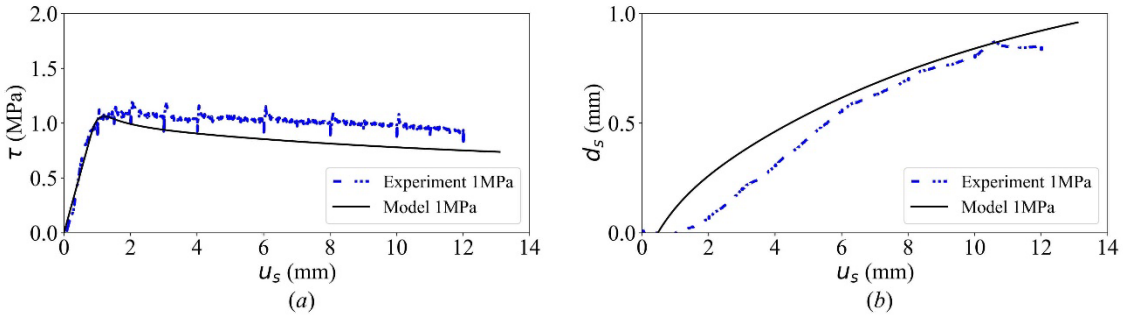

Figure 3. Comparison between the model simulation and measured (*a*) $\tau - u_s$, (b) $d_s - u_s$ of *S1*.

Figure 3 shows a comparison between the experimental and modelled shear behaviours at constant normal stresses of 1MPa. The shear stress rapidly rises until it reaches a peak value. After the peak, the shear stress gradually reduces due to the asperity wearing and shearing processes. Good agreement between the experimental results and model simulations has been presented with an average error of 15.8% for $\tau - u_s$ and 8.29% for $u_s - d_s$. However, a discrepancy between the experimental results and model simulations at the peak may be because of the early breakages of the critical asperities. In $u_s - d_s$ behaviours, the dilation increases with a gradually decreasing dilation gradient. The discrepancy between the proposed model and the experimental results in the initial gradient of $u_s - d_s$ plot is attributed to the sudden failure of joint asperities, which is not considered in the model.

Good agreements between the prediction and back-calculated e_h and Forchheimer's coefficients shown in Figure 4 (*a*) to (*c*) illustrate that Eqs. (4) and (5) can well describe the hydraulic behaviours of a fracture in a shear process. However, it is important to note that using different best-fit methods can lead to discrepancies between measured and simulated A and B.

To further validate the performance of the Forchheimer-based model, it is necessary to compare the measured and simulated flow discharges at σ_n= 1 MPa, as illustrated in Figure 4 (d). An average error of 10.88% indicates that the model can accurately capture the fracture hydraulic behaviours. It is important to note that this level of error is within an acceptable range for hydraulic models in nonlinear flow situations; thus, the model is a reliable tool for predicting the fracture flow rate.

4 CONCLUSION

This study proposes a novel hydromechanical model that comprises a multi-scale roughness shear model, a fracture void space model, and a Forchheimer-based flow model to describe the mechanical and hydraulic behaviours of a single fracture during shearing. The model estimates fracture shear behaviours using a wear theory-based approach in the shear model. Fracture void space evolutions are simulated in the fracture void space model and are then incorporated into the Forchheimer-based flow model. The apertures of the fracture are characterised by the mean and standard deviations of the local apertures. To consider the nonlinear flow behaviour induced by the fracture surface geometries, three parameters (ξ/e_h, ϑ, and T_s) are introduced into B. The model was validated through a series of shear-flow laboratory tests, conducted under injection water pressures ranging from 5 to 60 kPa and constant normal stresses of 1MPa. The prediction fracture discharges agree with the experimental measurements, which indicates that the model can accurately capture the hydromechanical behaviour of a single fracture.

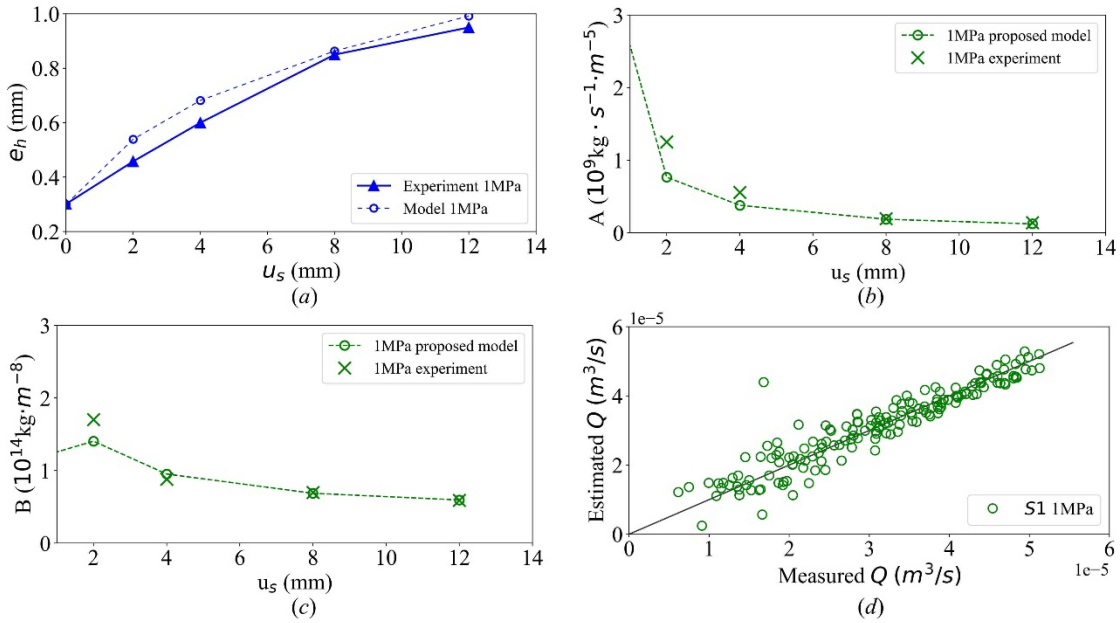

Figure 4. Comparison between the modelled and measured $(a) e_h - u_s$, $(b)\ A - u_s$, $(c)\ B - u_s$, $(d)\ Q$ of *S1*.

REFERENCES

Chen, Y., Zhou, J., Hu, S., Hu, R. & Zhou, C. 2015. Evaluation of Forchheimer equation coefficients for non-Darcy flow in deformable rough-walled fractures. *Journal of Hydrology,* 529**,** 993-1006.

Esaki, T., Du, S., Mitani, Y., Ikusada, K. & Jing, L. 1999. Development of a shear-flow test apparatus and determination of coupled properties for a single rock joint. *International Journal of Rock Mechanics and Mining Sciences,* 36**,** 641-650.

Gao, M., Zhang, C. & Oh, J. A multi-scale roughness shear joint model using wear theory. IOP Conference Series: Earth and Environmental Science, 2023. IOP Publishing, 012052.

Olsson, R. & Barton, N. 2001. An improved model for hydromechanical coupling during shearing of rock joints. *International Journal of Rock Mechanics and Mining Sciences,* 38**,** 317-329.

Rong, G., Yang, J., Cheng, L., Tan, J., Peng, J. & Zhou, C. 2018. A Forchheimer Equation-Based Flow Model for Fluid Flow Through Rock Fracture During Shear. *Rock Mechanics and Rock Engineering,* 51**,** 2777-2790.

Wang, C., Jiang, Y., Liu, R., Wang, C., Zhang, Z. & Sugimoto, S. 2020. Experimental study of the nonlinear flow characteristics of fluid in 3D rough-walled fractures during shear process. *Rock Mechanics and Rock Engineering***,** 1-24.

Witherspoon, P. A., Wang, J. S. Y., Iwai, K. & Gale, J. E. 1980. Validity of Cubic Law for fluid flow in a deformable rock fracture. *Water Resources Research,* 16**,** 1016-1024.

Xiong, X., Li, B., Jiang, Y., Koyama, T. & Zhang, C. 2011. Experimental and numerical study of the geometrical and hydraulic characteristics of a single rock fracture during shear. *International Journal of Rock Mechanics and Mining Sciences,* 48**,** 1292-1302.

Xiao, W., Xia, C., Wei, W., Bian, Y., 2013. Combined effect of tortuosity and surface roughness on estimation of flow rate through a single rough joint. J. Geophys. Eng., 10, doi: 10.1088/1742-2132/10/4/045015.